IOP PUBLISHING JOURNAL OF PHYSICS: CONDENSED MATTER

J. Phys.: Condens. Matter **21** (2009) 115702 (8pp) doi:10.1088/0953-8984/21/11/115702

Electronic excitations and their effect on the interionic forces in simulations of radiation damage in metals

C P Race, D R Mason and A P Sutton

Department of Physics, Imperial College London, London SW7 2AZ, UK

E-mail: chris.race06@imperial.ac.uk

Received 19 December 2008
Published 20 February 2009
Online at stacks.iop.org/JPhysCM/21/115702

Abstract

Using time-dependent tight-binding simulations of radiation damage cascades in a model metal we directly investigate the nature of the excitations of a system of quantum mechanical electrons in response to the motion of a set of classical ions. We furthermore investigate the effect of these excitations on the attractive electronic forces between the ions. We find that the electronic excitations are well described by a Fermi–Dirac distribution at some elevated temperature, even in the absence of the direct electron–electron interactions that would be required in order to thermalize a non-equilibrium distribution. We explain this result in terms of the spectrum of characteristic frequencies of the ionic motion. Decomposing the electronic force into four well-defined components within the basis of instantaneous electronic eigenstates, we find that the effect of accumulated excitations in weakening the interionic bonds is mostly (95%) accounted for by a thermal model for the electronic excitations. This result justifies the use of the simplifying assumption of a thermalized electron system in simulations of radiation damage with an electronic temperature dependence and in the development of temperature-dependent classical potentials.

(Some figures in this article are in colour only in the electronic version)

1. Introduction

Metals under fast neutron bombardment suffer damage at the atomic scale as a result of collision cascades. A neutron impinging on the surface transfers kinetic energy to a metal ion (the primary knock-on atom or PKA) and this ion goes on to collide with others, creating a highly disordered region known as a displacement spike [1]. Relaxation of the displacement spike results in a residual population of interstitial and vacancy defects, which influences the long-term microstructural evolution of the metal. Because the evolution of a collision cascade takes place on experimentally inaccessible picosecond timescales, simulation has been the primary means for establishing the damage produced in metals subjected to neutron bombardment. Most dynamical simulations over the last decade have employed classical molecular dynamics (MD) [2] and have thus treated the electrons of the target material only implicitly within some model for the interionic potential. It is expected that the electrons should, in fact, play an important role in the dynamics of radiation damage and several attempts have been made to incorporate their effects. Finnis *et al* [3], Nordlund *et al* [4] and Caro and Victoria [5] have all introduced a drag force into the ionic dynamics to account for energy loss to the electrons. Duffy and Rutherford [6] include a model of the electrons as a diffusive heatbath, exchanging energy with the underlying atomic subsystem via drag and stochastic forces. In the present paper we discuss the use of a model which goes beyond such phenomenological approaches by including the effect of electrons through explicit treatment of their dynamics.

We are applying semi-classical Ehrenfest dynamics [7] to a simple s-band tight-binding model of a metal [8] to simulate the evolution of a system of classical ions under the influence of forces due to electrons treated quantum mechanically. In turn the electrons, represented as a single-particle density matrix, are evolved under a tight-binding Hamiltonian that is parameterized by the positions of the ions. Details of our method can be found in [9] and [10]. Using our model we are able to explore the effect of energy transfer from ions to electrons on the development of a collision cascade.

The interionic forces in classical MD simulations implicitly assume the validity of the Born–Oppenheimer approximation. In contrast, the explicitly included electrons in our simulations have a finite response time to ionic motion (i.e. to changes in the electronic Hamiltonian) and we are able to monitor any effect that this has on the electronic forces between ions. We can identify two such possible effects. First, the finite response time of the electron density to movement of the ions may give rise to a non-conservative, non-adiabatic force on the ions. Models incorporating a classical drag force are attempting to capture this effect [3, 4, 6]. Second, as a collision cascade progresses, excitations will accumulate in the electronic system and may give rise to changes in the assumed conservative electronic forces between ions.

We have already begun to investigate the first of these effects [9] and have considered the validity of representing the energy loss to electrons via a drag term [10]. In this paper we will investigate the magnitude of the second effect and determine to what extent electronic excitation will alter the strength of interionic forces in collision cascades. By carrying out cascade simulations in which the dynamics of electrons are explicitly treated, we are able to assess the validity of the Born–Oppenheimer assumption implicit in the interatomic potentials used in classical MD simulations.

In section 2 we discuss a set of tight-binding simulations carried out with Ehrenfest dynamics and the results obtained. In section 3 we discuss the nature of the electronic excitations and consider ways to extrapolate our results beyond regimes accessible by direct simulation. In section 4 we offer our conclusions about the implications of the current work.

2. Investigation of electronic forces using Ehrenfest dynamics

2.1. A simple tight-binding model

We gather representative data on the electronic forces by simulating a series of collision cascades in our tight-binding model parameterized for copper [8]. We use the simplest possible electronic Hamiltonian, $\hat{H}$, given in the basis of atomic orbitals as

$$H_{IJ} = \gamma(|\mathbf{R}_I - \mathbf{R}_J|), \tag{1}$$

where I and J label non-overlapping s-orbitals centred on ions at positions $\mathbf{R}_I$ and $\mathbf{R}_J$, respectively. The hopping parameters γ vary as an inverse power of the interionic separation and are truncated between the ideal second and third nearest neighbour separations. The onsite elements of $\hat{H}$ are set to zero[1]. The electrons are represented as a single-particle density operator $\hat{\rho}$, and the ions also experience a pairwise repulsive force varying as an inverse power of their separation.

The electronic density operator is initialized according to a Fermi–Dirac distribution $f(\epsilon; T)$ at a temperature of $T(0) = 300$ K. We write such a density operator as

$$\hat{\rho}(0) = \sum_i f(\epsilon_i(0); T(0))\, |\phi_i(0)\rangle\, \langle\phi_i(0)|, \tag{2}$$

[1] As in [9] we find that including a self-consistent diagonal Hamiltonian matrix element of Hubbard U form has very little effect; the interionic charge transfers are in any case small (typically $\sim 0.01e$).

where $|\phi_i(0)\rangle$ is an eigenstate of the electronic Hamiltonian at time $t = 0$ and of energy $\epsilon_i(0)$. This density operator is evolved according to the quantum Liouville equation

$$\mathrm{i}\hbar \frac{\partial}{\partial t}\hat{\rho}(t) = \left[\hat{H}(\mathbf{R}; t), \hat{\rho}(t)\right], \tag{3}$$

where the electronic Hamiltonian $\hat{H}(\mathbf{R}; t)$ has an implicit time-dependence through its parameterization in terms of the ionic coordinates $\{\mathbf{R}_I(t)\}$, which from now on will be written collectively as $\mathbf{R}$. This evolution of the density operator is equivalent to the time-dependent Schrödinger equation for the evolution of the wavefunction. The classical ions are evolved under the pairwise repulsive force and an attractive electronic force depending on the density operator and the gradient of the electronic Hamiltonian with respect to the ionic positions. This electronic force will be

$$\mathbf{F} = -\mathrm{Tr}\,(\hat{\rho}\,\nabla\hat{H}), \tag{4}$$

where the gradient operator acts on the ionic positions.

2.2. The electronic force

We can gain insight into the electronic force by considering the time-evolved density operator $\hat{\rho}(t)$ of equation (3) in the basis of instantaneous eigenstates of the Hamiltonian at time t. Writing these eigenstates as $\{|\phi_i(\mathbf{R}; t)\rangle\}$ with eigenvalues $\{\varepsilon_i(\mathbf{R}; t)\}$ we have

$$\hat{\rho}(t) = \sum_{i,j} |\phi_i(\mathbf{R}; t)\rangle\, \rho_{ij}(t)\, \langle\phi_j(\mathbf{R}; t)| \tag{5}$$

which defines the matrix elements $\rho_{ij}(t)$. In this basis, equation (4) becomes

$$\mathbf{F}(t) = -\sum_i \rho_{ii}(t)\nabla\varepsilon_i(\mathbf{R}; t) - \sum_{i,j,i\neq j} (\varepsilon_i(\mathbf{R}; t) - \varepsilon_j(\mathbf{R}; t))\rho_{ij}(t)\, \langle\phi_j(\mathbf{R}; t)|\nabla\phi_i(\mathbf{R}; t)\rangle. \tag{6}$$

The first term represents the motion of the ions on a collection of potential energy surfaces of the eigenvalues weighted according to the diagonal elements ρ_{ii}. The second term represents the effect of non-adiabaticity, where the matrix elements $\langle\phi_j(\mathbf{R}; t)|\nabla\phi_i(\mathbf{R}; t)\rangle$ are known as the non-adiabatic coupling vectors [11]. The diagonal elements ρ_{ii} contain information about the excitations that accumulate in the electronic system as a result of the ionic motion. We can separate out these excitations by considering the form that the density operator would take if the ions had traversed their trajectories infinitely slowly. Because the lack of symmetry in our Hamiltonian will eliminate crossings and accidental degeneracies of the eigenstates, adiabatic evolution will take an initial eigenstate of the Hamiltonian into the corresponding eigenstate (in an energy ordered list) at a later time t. We can therefore write the adiabatic density operator by holding the occupations of the eigenstates fixed at their initial values, $\rho_{ii}(t = 0)$. For our chosen initialization we have

$$\hat{\rho}^0(\mathbf{R}; t) = \sum_i |\phi_i(\mathbf{R}; t)\rangle\, f(\varepsilon_i(0); T(0))\, \langle\phi_i(\mathbf{R}; t)|. \tag{7}$$

Experiment suggests that an excited electronic system should thermalize to a well defined temperature on a timescale of ∼10–100 fs [12]. Anticipating that the excited density matrix elements $\rho_{ii}(t)$ will have an approximately thermal character, we can define a third density operator in which the eigenvalues are occupied according to a characteristic temperature $T(t)$:

$$\hat{\rho}^T(\mathbf{R};t) = \sum_i |\phi_i(\mathbf{R};t)\rangle\, f(\varepsilon_i(\mathbf{R};t);T(t))\,\langle\phi_i(\mathbf{R};t)|. \quad (8)$$

We quantify the error involved in making this approximation later. Separating out the various components of the density operator as $\hat{\rho} = \hat{\rho}^0 + (\hat{\rho}^T - \hat{\rho}^0) + (\hat{\rho} - \hat{\rho}^T)$ allows us to rewrite the electronic force in equation (6) as

$$\begin{aligned}\mathbf{F} = &-\sum_i f(\varepsilon_i(0);T(0))\nabla\varepsilon_i(\mathbf{R};t)\\ &-\sum_i \{f(\varepsilon_i(\mathbf{R};t);T(t)) - f(\varepsilon_i(0);T(0))\}\nabla\varepsilon_i(\mathbf{R};t)\\ &-\sum_i \{\rho_{ii}(t) - f(\varepsilon_i(\mathbf{R};t);T(t))\}\nabla\varepsilon_i(\mathbf{R};t)\\ &-\sum_{i,j,i\neq j}(\varepsilon_i(\mathbf{R};t)-\varepsilon_j(\mathbf{R};t))\rho_{ij}(t)\langle\phi_j(\mathbf{R};t)|\nabla\phi_i(\mathbf{R};t)\rangle.\end{aligned} \quad (9)$$

For convenience we will refer to the four sum terms in equation (9) as $\mathbf{f}_1$, $\mathbf{f}_2$, $\mathbf{f}_3$ and $\mathbf{f}_4$ respectively. $\mathbf{f}_1$ is the adiabatic force that would be exerted on the ions if they had followed their trajectories infinitely slowly. $\mathbf{f}_2$ represents the effect of excitations characterized by a temperature $T(t)$ and $\mathbf{f}_3$ is a correction to those excitations due to the occupations of the eigenstates at time t not being exactly thermally distributed. Their sum, $\mathbf{f}_2 + \mathbf{f}_3$, gives the total effect of accumulated electronic excitations on the conservative forces. By contrast, $\mathbf{f}_4$ is a dynamic term, giving the non-conservative contribution due to the finite response time of the density matrix to ionic motion. Simulations of radiation damage cascades using MD incorporating a drag force on the ions can be viewed as attempts to incorporate the effects of $\mathbf{f}_4$.

As a cascade evolves, the work done by the force $\mathbf{f}_4$ will appear as excitations in the density matrix, in the quantities $\rho_{ii} - \rho^0_{ii}$. The forces $\mathbf{f}_1$, $\mathbf{f}_2$ and $\mathbf{f}_3$ are conservative when these excitations are taken into account. We can measure the size of this non-adiabatic energy transfer from ions to electrons by considering the excess of energy in the system with the time-evolved density matrix compared with the adiabatic density matrix $\hat{\rho}^0$. We write this as

$$\Delta E = \mathrm{Tr}\left((\hat{\rho} - \hat{\rho}^0)\hat{H}\right). \quad (10)$$

As more and more energy enters the electronic system, the bonding interactions will be reduced and we should see an increasingly repulsive interaction between ions. This force, $\mathbf{f}_2 + \mathbf{f}_3$, is absent in the case of classical MD simulations in which the interaction potential remains constant for the duration of the cascade. It is an aim of the current work to quantify the effect of this omission.

2.3. Simulations results

We have generated cascade data, including electronic excitations and forces, for a set of forty-four simulations with the initial PKA direction evenly distributed over the irreducible solid angle of $4\pi/48$ steradians associated with the fcc unit cell [13]. In each case, a simulation cell of 2016 atoms ($9 \times 7 \times 8$ face-centred cubic (fcc) unit cells) with periodic boundary conditions is set up and allowed to thermalize to an ionic temperature of 300 K over 1 ps of classical MD with a Sutton–Chen potential [14] and 100 fs of Born–Oppenheimer dynamics under the tight-binding Hamiltonian. The density operator is initialized to an electronic temperature of 300 K. We then impart 2 keV of kinetic energy to one ion, our PKA, in a particular direction and allow the system to evolve under Ehrenfest dynamics. The simulations are allowed to run for 225 fs,[2] with a timestep of 0.01 fs. In a typical simulation the total energy transfer to the electrons will be around 45 eV, or 22 meV per electron. Over 75% of the ions will have been displaced by more than 0.5 Å from their perfect lattice sites at some point during the cascade and the cascades overlap the periodic boundaries.

We compute a double histogram as the simulations progress, in which each atom pair is binned according to the spacing and the bond-order between the ions. We then determine the average electronic bond force (a product of the bond-order and the gradient of the hopping parameter) corresponding to the midpoint of each histogram bin. Generating these histograms at intervals throughout the simulation for the three density matrices defined above allows us to determine the effect of electronic excitation on the components of the electronic force in equation (9) within the simulation cell.

By averaging the bond-order data from the histogram output over all atom pairs with a given separation and over all simulations we can obtain an ensemble averaged electronic bond force as a function of separation (indicated below by angle brackets). Figure 1 shows these force curves for the mean excited electronic force, $\langle|\mathbf{F}|\rangle = \langle|\mathbf{f}_1 + \mathbf{f}_2 + \mathbf{f}_3 + \mathbf{f}_4|\rangle$ (calculated using $\hat{\rho}$), for the point in the simulations at which $\Delta E \approx 43$ eV. Also shown is the reduction in the mean attractive electronic force, $(\langle|\mathbf{f}_1|\rangle - \langle|\mathbf{F}|\rangle)/\langle|\mathbf{f}_1|\rangle$, where $\langle|\mathbf{f}_1|\rangle$ is the mean adiabatic force (calculated using $\hat{\rho}^0$). There is a clear weakening of bonds, but the effect is small (about 0.4%) for the degree of electronic excitation achieved in these cascades.

3. Extrapolating the results

3.1. A thermal model for the electronic excitations

The computational constraints on the size and duration of the cascades that we can simulate place a low limit on the amount of energy that we can inject into the electronic system by direct simulation. The 2 keV of kinetic energy in the cascades considered is low; we would expect PKA energies of several tens of kilo electron volt to be more typical. We therefore seek a valid means of extrapolating

[2] Such a simulation, including the thermalization, typically takes 72 h on a 2.66 GHz processor.

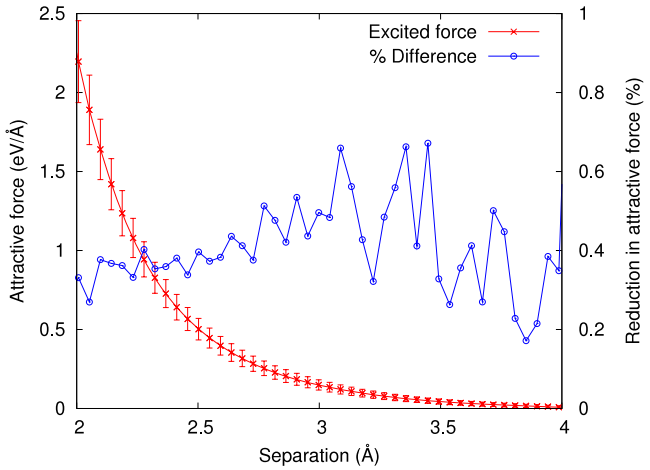

Figure 1. The strength of the attractive electronic force between ion pairs as a function of the interionic separation. The data are shown for the time-evolved density operator corresponding to $\langle|\mathbf{f}_1+\mathbf{f}_2+\mathbf{f}_3+\mathbf{f}_4|\rangle$ (crosses). Data for the adiabatic density operator corresponding to $\langle|\mathbf{f}_1|\rangle$ are indistinguishable from these at this scale. Variations in the local atomic environments give a spread in the force at a given separation and the error bars show the standard deviation of this spread. The right-hand vertical axis shows the expectation of the percentage difference between the two forces (circles).

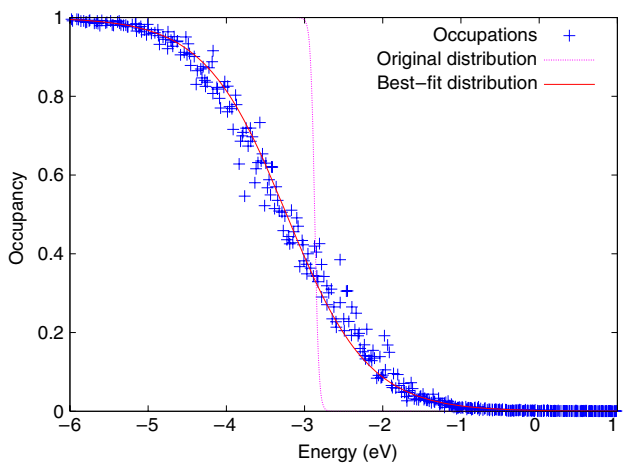

Figure 2. The population of the instantaneous eigenstates for a typical simulation after 225 fs, when the cascade region fills the simulation volume. A Fermi–Dirac distribution corresponding to the original temperature of 300 K is shown, along with a Fermi–Dirac function corresponding to a temperature of 6055 K as a best fit to the excited occupation distribution.

our results to higher electronic excitations. Figure 2 shows a plot of the occupation of the instantaneous eigenstates after 225 fs of a typical simulation (i.e. a plot of $\rho_{ii} \equiv \langle\phi_i(\mathbf{r};t)|\hat{\rho}(t)|\phi_i(\mathbf{r};t)\rangle$ as a function of $\epsilon_i(\mathbf{r};t)$) and we can see that the occupancy function looks thermal with a temperature of 6055 ± 48 K. The fact that the excited electrons appear to have a thermal distribution suggests a convenient means of extrapolating the degree of excitation—by simply further heating the electrons.

At first sight this result is surprising. Our simulations do not incorporate the direct electron–electron interactions that would allow a non-equilibrium distribution of electrons to thermalize. The excitations occurring during the cascade must therefore directly yield a thermal distribution at an elevated temperature. This makes sense if the final distribution is viewed as the cumulative result of many excitations, all small on the scale of $2k_BT$, the width of the Fermi–Dirac function, where T is the final electronic temperature. If all the electronic excitations are small jumps, the evolution of the occupancy function will be a one-dimensional diffusion in energy space and it is the similarity of the solution of the diffusion equation where the initial condition is a step function (namely the complementary error function) to the Fermi–Dirac function which maintains a thermal-looking distribution of the electrons.

We can estimate an upper kinetic energy bound for the ions to produce a thermal-looking electronic distribution as follows: if we consider the characteristic frequency of an ion moving with speed v to be $\omega = 2\pi v/b$ where b is some typical impact parameter (say the nearest neighbour distance) and associate a transition energy $\hbar\omega$ with the ionic motion then we can calculate the condition on the ion kinetic energy for a given electronic temperature, corresponding to $\hbar\omega \ll k_BT$:

$$K \ll \frac{M}{2}\left(\frac{k_BTb}{2\pi\hbar}\right)^2, \tag{11}$$

where M is the ion mass. For our copper ions, with $b = 2.6$ Å, a temperature of 5000 K corresponds to a condition on the ion kinetic energy of $K \ll 233$ eV. This seems small compared to the initial 2 keV, but this kinetic energy will be rapidly shared amongst several hundred ions and we expect the condition for diffusive evolution of the occupancy function to be satisfied during the simulation, except for the first few collisions.

We can test the assertion that the excited electronic distribution is thermal by attempting to fit a Fermi–Dirac distribution to our simulation data. This is most easily accomplished using a simple linear regression of $\ln(1/\rho_{ii}-1)$ against $\varepsilon_i - \mu$ for each set of occupations, where ρ_{ii} is the fractional occupancy of the eigenstate of energy ε_i. μ is the chemical potential corresponding to the fitted temperature and satisfying the condition that the system is neutral. The gradient of the regression line will be $1/k_BT$. The temperature fitting algorithm used is described in more detail in the appendix. Figure 3 shows the fitted temperatures for our set of forty-four 2 keV simulations every 10 fs (a total of 1012 datapoints). R^2 measures of the goodness of fit for the regression are typically around 0.95 and the fitted temperatures show very good agreement between simulations, suggesting that the energy transfer is well described by thermal distributions. There is also good agreement with the theoretical curve for an electronic heat capacity based on the Sommerfeld expansion for the free electron gas [15][3], lending further support for the thermal model.

In the early stages of each simulation, an insufficient number of electronic excitations will have occurred for a good

[3] $c_v = (\pi^2/3)k_B^2Tg(\varepsilon_F)$, where $g(\varepsilon_F)$ is the density of states at the Fermi level. We expect the free electron result to be valid for our tight-binding model because it has a low band-filling and a nearly spherical Fermi surface.

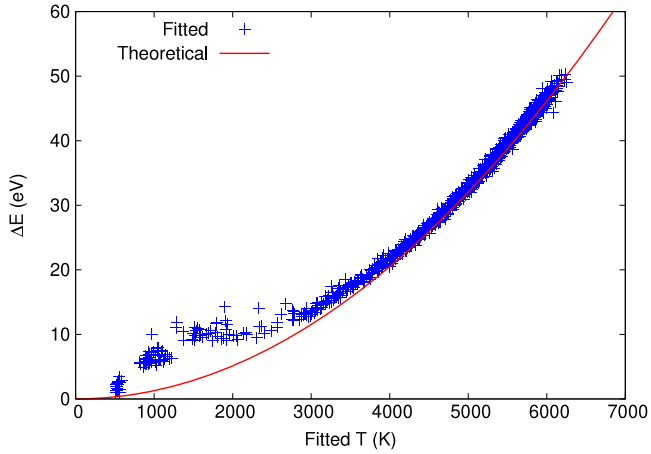

Figure 3. Plot of ΔE (equation (10)) against fitted temperature for forty-four 2 keV simulations. The solid line indicates the theoretical curve for the electronic heat capacity based on the Sommerfeld expansion. The deviation from the theoretical line is discussed in the main text. The fitting algorithm is described in the appendix.

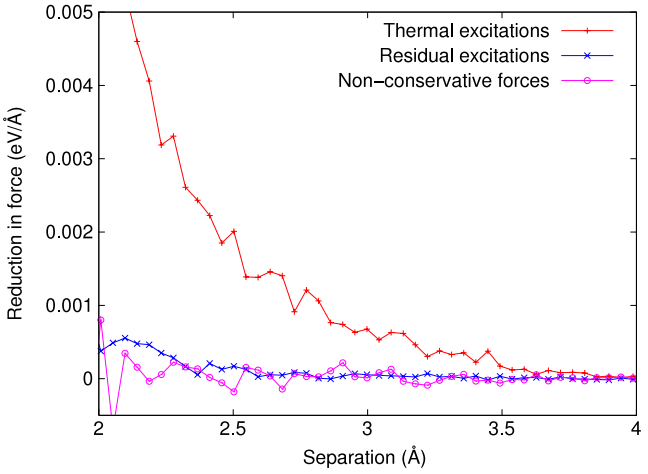

Figure 4. The reduction in the mean attractive electronic force as a function of pairwise separation due to the neglect of the various components of the electronic force defined in section 2: the effect of thermal excitations, $\langle|\mathbf{f}_1+\mathbf{f}_2|\rangle - \langle|\mathbf{f}_1|\rangle$ (vertical crosses), the effect of excitations not captured by the thermal model, $\langle|\mathbf{f}_1+\mathbf{f}_2+\mathbf{f}_3|\rangle - \langle|\mathbf{f}_1+\mathbf{f}_2|\rangle$ (diagonal crosses) and the effect of the non-conservative forces, $\langle|\mathbf{f}_1+\mathbf{f}_2+\mathbf{f}_3+\mathbf{f}_4|\rangle - \langle|\mathbf{f}_1+\mathbf{f}_2+\mathbf{f}_3|\rangle$ (circles).

thermal distribution to have been established. Therefore the fit to the theoretical curve at low excitation is less good, although the deviation is similar across all simulations. After just 5 fs the small number of excitations is sufficient only to disrupt the initial Fermi–Dirac distribution and the temperature fitting algorithm fails to generate a temperature in 55% of cases. By 15 fs a satisfactory fit is always achieved.

Excitations created by ionic motion will initially be spatially localized, spreading on a timescale set by the electronic thermal conductivity. In an N atom system this spreading takes place on a timescale of order $N^{1/3}\gamma/h$ and the excitations can be considered to be delocalized over the whole volume within ∼6 fs. Future simulations with larger systems may show an effective temperature gradient around the cascade region.

Figure 1 showed the effect of electronic excitation on the average interionic force as function of pairwise separation. By fitting a temperature to the excited electron distributions in our simulations, we can construct $\hat{\rho}^T(\mathbf{R};t)$ and compare the contributions $\mathbf{f}_2$ through to $\mathbf{f}_4$ to the force between pairs of ions. Figure 4 shows that the majority (∼95%) of the effect of electronic excitation on the pairwise force is captured by the thermal model in the component $\mathbf{f}_2$, the effect of the residual excitations in the full density matrix (which give rise to $\mathbf{f}_3$) being small. It should be noted that whilst the dynamic term $\mathbf{f}_4$ contributes little when averaged over pairwise interactions (because its direction is not correlated with the bonds), its magnitude is significant when considered on an atom by atom basis. $|\mathbf{f}_4|$ for a given atom will tend to scale with the ionic velocity [10], whereas $|\mathbf{f}_2|$ will scale with the degree of electronic excitation. We would therefore expect that on average $|\mathbf{f}_2|$ will grow from zero over the course of the simulation, whereas $|\mathbf{f}_4|$ will depend on the distribution of ion velocities. Towards the end of our 225 fs simulations the two components have similar orders of magnitude.

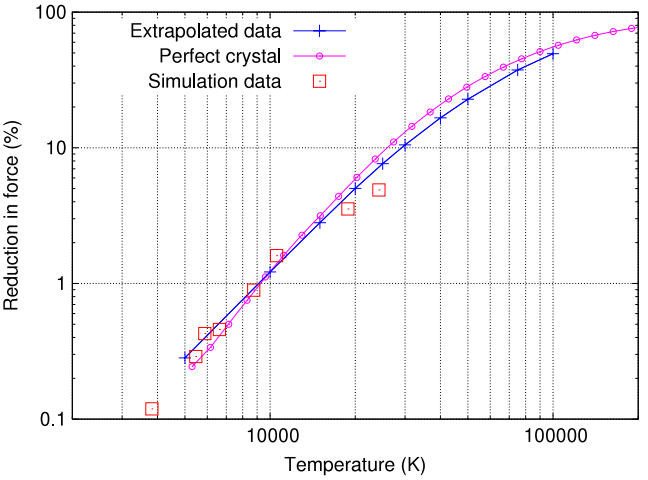

Figure 5. Extrapolation of the effect of electronic excitation on the attractive electronic force. Three methods of extrapolation are shown: (1) imposing the elevated temperature given on the horizontal axis on ionic configurations taken from the initial simulations (crosses). (2) The results of further dynamical simulations at higher PKA energies up to 50 keV (boxes). (3) Calculations based on the effect of electronic temperature on the bond orders in a perfect crystal (circles).

3.2. High temperature results

Given that a thermal model captures well the effect of electronic excitations on the interionic forces we can extrapolate our simulation results by elevating the electronic temperature and recalculating the forces. Figure 5 shows the reduction in the attractive electronic force as a function of electronic temperature calculated in three different ways.

We first take the ionic positions from the end of each of our set of 44 simulations and impose an elevated electronic temperature. The simulation results are simply used to provide

a sample of distorted ionic configurations for which we can examine the various contributions to the electronic forces and these points are not therefore representative of simulations which might reach such a high temperature.

Second, we carry out further sets of simulations at higher PKA energies of 5, 20 and 50 keV and calculate the forces. At these higher energies the cascade front will cross the periodic boundaries of the simulation cell very early on, but we can once again view the simulation merely as a means of generating distorted ionic configurations.

As a third method of extrapolating our results, we consider the effect of an elevated electronic temperature on the nearest and next-nearest neighbour bond-orders within our tight-binding model in a perfect lattice. In a real cascade the region of electronic excitation will extend far beyond the cascade front, due to the high electronic thermal conductivity. We would therefore expect electronic excitations to affect a region of undistorted lattice surrounding the cascade.

The data for the three methods of extrapolation lie on the same curve and we can see that significant reductions of the attractive electronic force of order 10% would occur at high electronic temperatures of 3×10^4 K.

4. Conclusions and discussion

A set of simulations of radiation damage cascades using Ehrenfest dynamics in a tight-binding model of copper allows us to calculate the effect of electronic excitations on the attractive forces between ions. We find that the excitations themselves are well described by a Fermi–Dirac distribution at some elevated temperature and that this best-fit temperature coincides well with that calculated from the total non-adiabatic energy transfer using the Sommerfeld form for the electronic heat capacity. A decomposition of the electronic force in the basis of instantaneous electronic eigenstates (see equation (9)) demonstrates that a thermal model also captures over 95% of the reduction in the attractive electronic force due to the full spectrum of excitations. Extrapolating our results to higher electronic temperatures predicts the effect of higher levels of electronic excitation on the electronic forces between ions.

The significance of our results depends on the electronic temperatures developed in real cascades. Whilst such cascades will typically involve PKA energies of several tens of kilo electron volts, we note that our simulation and extrapolated results are all derived under periodic boundaries in a small cell. In reality, the energy injected into the electrons by the ionic motion would be rapidly dispersed due to the high electronic thermal conductivity. The balance between the rate of energy injection by the cascade and the dispersion of the energy within the electron gas will determine the electronic temperature distribution as a function of time and hence the extent to which the electronic forces are modified.

Duffy *et al* [16, 17] have developed a model combining a classical MD simulation of ionic evolution with a model of electrons as an inhomogeneous heatbath evolving according to the heat diffusion equation. This model allows them to determine the spatial distribution of electronic temperature during simulations of collision cascades. In [17] they find maximum electronic temperatures of up to 7000 K in 10 keV cascades. Their results are highly sensitive to the assumed coupling between ions and electrons in the model and literature estimates for this parameter [3, 18, 19] vary by several orders of magnitude.

One way to include the effects of electronic excitation on conservative forces in a classical molecular dynamics simulation, in which all the interactions are described by a potential, would be to make that potential dependent on the local electronic temperature. Given the lack of an unambiguous estimate for the maximum electronic temperature attained in real radiation damage cascades in metals, the need for such a potential remains an open question. If cascades are able to cause a rise in temperature to above 10^4 K then it is possible that the effect on the interionic forces (a reduction in the electronic attractive force of over 1%) would cause a significant change to the ion dynamics. Furthermore, in higher energy events such as ion implantation by channelling, we might expect still higher electronic temperatures to be attained [16] and the need for a temperature-dependent force model is increased correspondingly.

Even in situations where electronic temperatures reach only 5000 K, as in our 2 keV simulations, we might need to take account of the reduction in the attractive electronic force. A region surrounding the collision cascade and bathed in the excited electron gas will experience reduced bonding interactions between ions and can be regarded as an inclusion under compressive stress. An apparently small decrease in the bonding interaction of $\sim$0.4% implies a significant effective volume strain of $\sim$0.2% on the inclusion. A strain of this magnitude, whilst short-lived, could give rise to an outward propagating elastic wave, which might need to be taken into account when considering the evolution of the damage distribution.

Development of a potential with a dependence on electronic excitation is greatly simplified if a Fermi–Dirac distribution can be assumed (see [20] for an example). Whilst in real cascades electron–electron interactions will drive the excitations towards a thermal distribution, the timescale for this thermalization (10–100 fs) is comparable to the timescale of the cascade evolution. These simple considerations do not lead us to expect the assumption of a well established electronic temperature to be valid. However, our simulations demonstrate that even in the absence of direct electron–electron interactions, the nature of the excited electronic spectrum is well modelled by a thermal distribution, because the characteristic frequencies of the ionic motion are small on the scale of $k_B T$. The need for thermalization of strongly non-equilibrium electronic excitations never arises and the simplifying assumption of a well established electronic temperature may thus be made.

Acknowledgments

We thank Mike Finnis, Matthew Foulkes, Andrew Horsfield, Jonathan le Page and Sascha Khakshouri for useful discussions and Imperial College High Performance Computing Service for computing resources.

CPR and DRM were supported by EPSRC grant number EP/C524403.

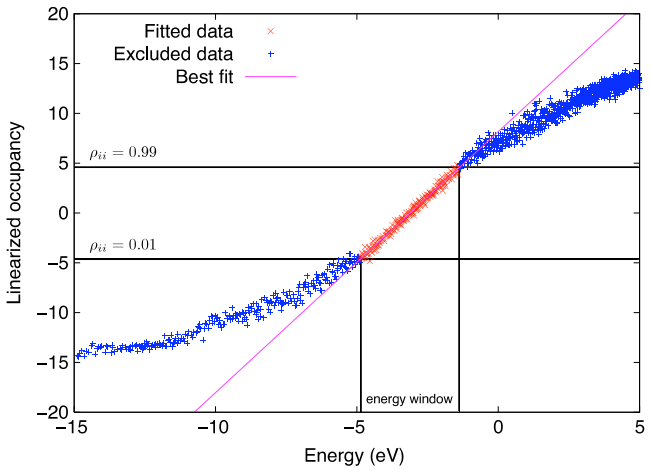

Figure A.1. A sample temperature fit to the eigenvalue occupations 100 fs into a 2 keV simulation. In this case the best fit is achieved by exploiting the largest fitting window allowed by our algorithm. The excluded data points in the non-linear tails are shown as (blue) vertical crosses. The 174 data points included in the fit are shown as (red) diagonal crosses. The best-fit temperature line ($T = 4429 \pm 40$ K, $\mu(T) = -3.116$ eV) is shown by the diagonal (purple) line.

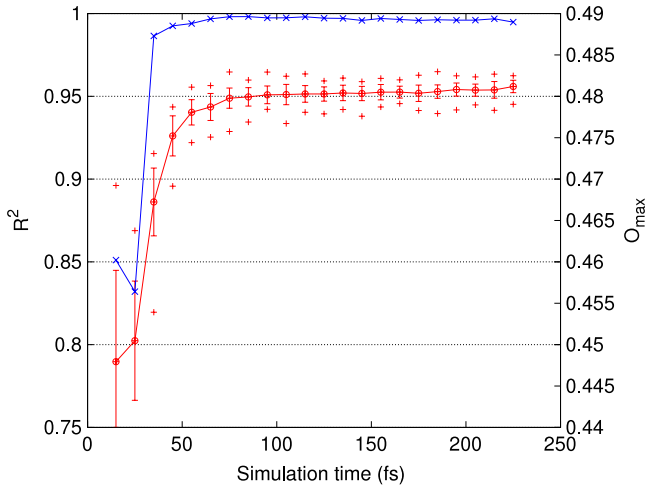

Figure A.2. The behaviour and performance of the temperature fitting algorithm for a set of forty-four 2 keV cascade simulations as a function of simulation time. (Red) circles show the mean of the distribution of R^2 across all simulations at a particular time. The error bars show the standard deviation and the (red) vertical crosses indicate the maximum and minimum R^2 within the set of simulations. The (blue) diagonal crosses show how the value of the parameter O_{max} for the optimum fit varies with time.

Appendix. Temperature fitting algorithm

We require an algorithm to generate a best-fit temperature for a set of occupations ρ_{ii} of a set of energy eigenstates with eigenvalues ε_i. We can write the Fermi–Dirac distribution in a linearized form as

$$\left|\ln\left(\frac{1}{f(\varepsilon;T)} - 1\right)\right| = \frac{1}{k_B T}|(\varepsilon - \mu(T))|, \qquad (A.1)$$

where for numerical convenience we have taken the absolute values of both sides. Applying a similar transformation to our eigenstate occupancy data (plotting $|\ln[(1/\rho_{ii}) - 1]|$ against $|\varepsilon_i - \mu(T)|$) allows us to use the standard tools of linear regression to obtain an estimator for the inverse temperature[4]. Because the chemical potential μ is a function of the fitted temperature, our algorithm incorporates a self-consistency loop. We first calculate an initial fitting temperature $T_1(\mu_0)$ for an initial estimate of the chemical potential μ_0. A new chemical potential $\mu_1(T_1)$ can then be calculated and used to obtain a revised estimate for the temperature $T_2(\mu_1)$. This procedure is repeated until consecutive temperatures agree to within a single degree. Because μ varies only slowly with temperature, convergence is achieved very quickly (typically within three iterations).

We have found that the nature of the electronic excitations in our simulations is such that it is best to restrict the energy range of the eigenvalues over which the fitting is carried out (see figure A.1). Early in the simulation the presence of high frequencies in the characteristic spectrum of the ionic motion causes excitations across the full width of the electron band. These excitations manifest themselves as deviations from linearity in the linearized occupation data which remain even when later excitations have generated a well established thermal-looking distribution over a narrower energy range about the Fermi energy. Except for very early in the simulation, the non-linear tails represent a small and decreasing proportion of the total electronic excitation and we choose to exclude them from the regression analysis in order to avoid overestimating the best-fit electronic temperature.

We begin by calculating a best-fit temperature for those data which fall within an energy window $|\varepsilon_i - \mu(T)| < E_{max}$ where we find that $E_{max} = 0.2$ eV provides enough data to obtain a valid initial fit. We then gradually increase the size of the energy window by increasing E_{max}, repeatedly recalculating the best-fit temperature, up to a maximum width corresponding to $|f(E_{max};T) - 0.5| < O_{max}$. The occupancy bound O_{max} is chosen to admit as many data as possible into the fitting window without incurring the risk that the non-linear tails will corrupt the fit. In practice we have found that a good value is $O_{max} = 0.49$. From the sequence of fitted temperatures we then choose that for which the R^2 measure of goodness of fit was the highest.

For our set of simulations of 2 keV cascades we have typically found that the optimum fitting range grows with time so that by around 35 fs we are using the maximum fitting window (see figure A.2). At earlier times, when the temperature is lower, a smaller fitting window is preferred. Typical values for R^2 are 0.94–0.965 as shown in figure A.2.

[4] Problems with the divergence of the linearized occupancy at $\rho_{ii} = 0$ and $\rho_{ii} = 1$ are avoided by restricting the range of fitted data, as discussed below.

References

[1] Averback R S and Diaz de la Rubia T 1997 Displacement damage in irradiated metals and semiconductors *Solid State Phys.* **51** 281–402

[2] Malerba L 2006 Molecular dynamics simulation of displacement cascades in α-Fe: a critical review *J. Nucl. Mater.* **351** 28–38

[3] Finnis M W, Agnew P and Foreman A J E 1991 Thermal excitation of electrons in energetic displacement cascades *Phys. Rev.* B **44** 567–74
[4] Nordlund K, Wei L, Zhong Y and Averback R S 1998 Role of electron–phonon coupling on collision cascade development in Ni, Pd, and Pt *Phys. Rev.* B **57** R13965–8
[5] Caro A and Victoria M 1989 Ion–electron interaction in molecular-dynamics cascades *Phys. Rev.* A **40** 2287–91
[6] Duffy D M and Rutherford A M 2007 Including the effects of electronic stopping and electron–ion interactions in radiation damage simulations *J. Phys.: Condens. Matter* **19** 016207
[7] Delos J B, Thorson W R and Knudson S K 1972 Semiclassical theory of inelastic collisions. I. Classical picture and semiclassical formulation *Phys. Rev.* A **6** 709–20
[8] Sutton A P M, Todorov T N, Cawkwell M J and Hoekstra J 2001 A simple model of atomic interactions in noble metals based explicitly on electronic structure *Phil. Mag.* A **81** 1833–48
[9] Mason D R, le Page J, Race C P, Foulkes W M C, Finnis M W and Sutton A P 2007 Electronic damping of atomic dynamics in irradiation damage of metals *J. Phys.: Condens. Matter* **19** 436209
[10] le Page J, Mason D R, Race C P and Foulkes W M C 2009 How good is damped molecular dynamics as a method to simulate radiation damage in metals? *New J. Phys.* **11** 013004
[11] Tully J C 1990 Molecular dynamics with electronic transitions *J. Chem. Phys.* **93** 1061–71
[12] Bennemann K H 2004 Ultrafast dynamics in solids *J. Phys.: Condens. Matter* **16** R995–1056
[13] le Page J 2008 The transfer of energy between electrons and ions in solids *PhD Thesis* Imperial College, London (Condensed Matter Theory Group, The Blackett Laboratory, Imperial College, London)
[14] Sutton A P and Chen J 1990 Long-range Finnis–Sinclair potentials *Phil. Mag. Lett.* **61** 139
[15] Ashcroft N W and Mermin N D 1976 *Solid State Physics* (Stamford, CT: Thomson Learning)
[16] Duffy D M, Itoh N, Rutherford A M and Stoneham A M 2008 Making tracks in metals *J. Phys.: Condens. Matter* **20** 082201
[17] Rutherford A M and Duffy D M 2007 The effect of electron–ion interactions on radiation damage simulations *J. Phys.: Condens. Matter* **19** 496201
[18] Wang Z G, Dufour C, Paumier E and Toulemonde M 1994 The S_e sensitivity of metals under swift-heavy-ion irradiation: a transient thermal process *J. Phys.: Condens. Matter* **6** 6733–50
[19] Ziegler J F, Biersack J P and Littmark U 1985 *The Stopping and Range of Ions in Solids* (Oxford: Pergamon)
[20] Khakshouri S, Alfè D and Duffy D M 2009 Development of an electron-temperature dpependent interatomic potential for molecular dynamics simulations of tungsten under electronic excitation *Phys. Rev.* B **78** 224304